Multiple abrupt phase transitions in urban transport congestion

Supplemental Material

Aniello Lampo[1], Javier Borge-Holthoefer[1], Sergio Gómez[2], Albert Solé-Ribalta[1,3]

[1]Internet Interdisciplinary Institute (IN3), Universitat Oberta de Catalunya, Barcelona, Catalonia, Spain
[2]Departament d'Enginyeria Informàtica i Matemàtiques, Universitat Rovira i Virgili, Tarragona, Catalonia, Spain
[3]URPP Social Networks, University of Zurich, Zurich, Switzerland

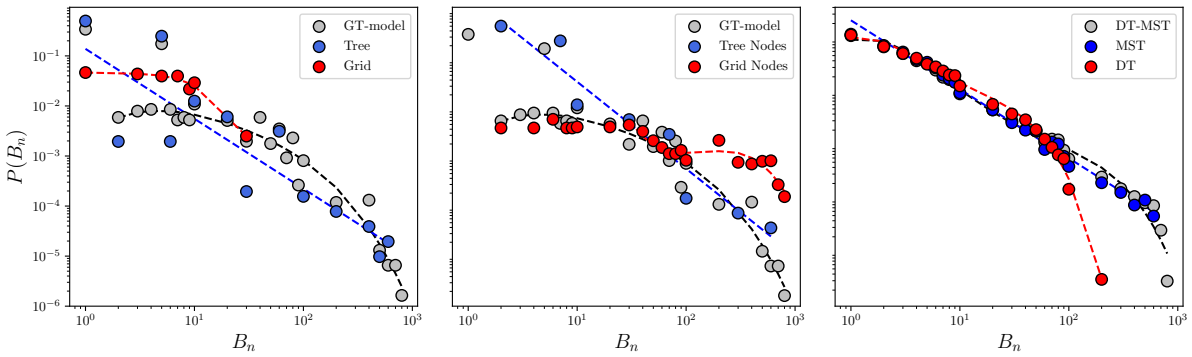

Figure S1: Betweenness distribution comparison of the GT-model, DT-MST, and the related null models: grid, tree, DT and MST. Left: A GT-model with $w = 45$, $h = 10$, and $r = 2$ is compared with its individual components, i.e., a grid with $w = 45$, and a tree with $h = 10$, $r = 2$. Middle: The same GT-model is compared with the betweenness distribution resulting from its grid and tree nodes. Right: A DT-MST model (obtained from the GT-model above, according the procedure explained in Sec. VI, and with $\Delta N/N = 1$) is compared with its underlying DT and MST structures. In all the cases, the betweenness values are normalized by the number of nodes. Dashed lines represent the resulting polynomial fit and highlight the cut-off role of the grid/DT and the damping one of the trees. In the left and right plots, the null models refer to independent graphs, while in the center we consider the grid and tree node contributions to the same GT-model network.

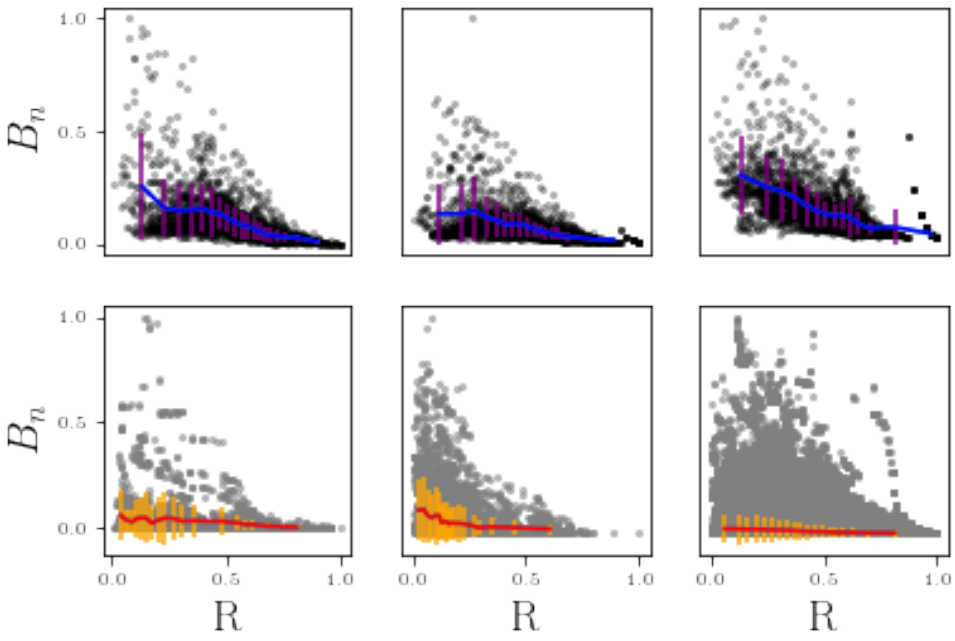

Figure S2: Comparison between the real (bottom) and estimated (top) relationship between nodes geographic position and their betweenness for small (Dalian, China), medium (Medan, Indonesia) and big cities (Tokyo, Japan), from the left to the right. The GT-models used have parameters $w = 51$, $r = 2$, $\Delta\rho/\rho = 1.5\%$, and $h = 1, 3, 5$ from the left to the right. All distances and betweenness are normalized between 0 and 1. Coordinates for the nodes of the GT-model have been assigned using the planar embedding described in Appendix A1. Solid lines on the scatter plots represent the mean betweenness at the given radius R. Deviations correspond to one σ of the distribution.

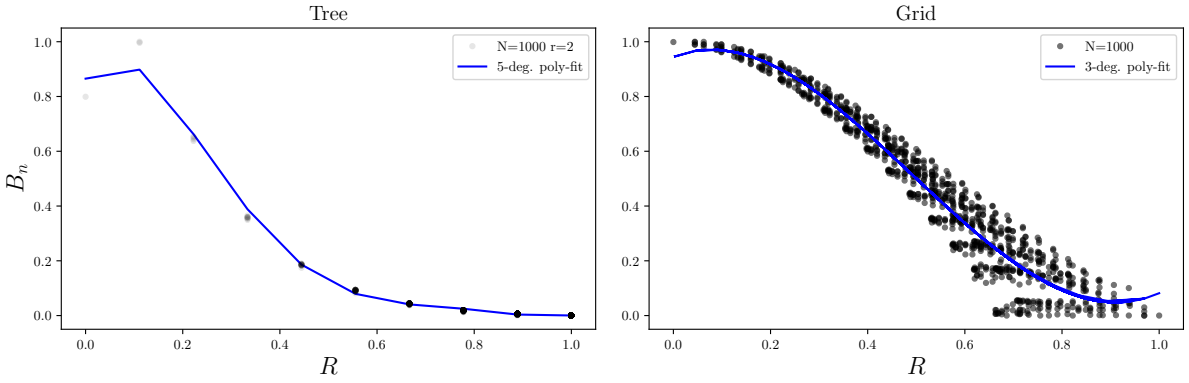

Figure S3: Spatial behavior of the betweenness centrality for a tree (left) and a grid (right). Each point represents a node, and its horizontal and vertical coordinates correspond to its betweenness and geographic position, respectively. In the case of the grid, geographic position is defined as the euclidean distance from its geometric center, while it refers to the number of jumps from its root in the case of the tree. The blue line portrays a polynomial fit of the betweenness radius behavior.

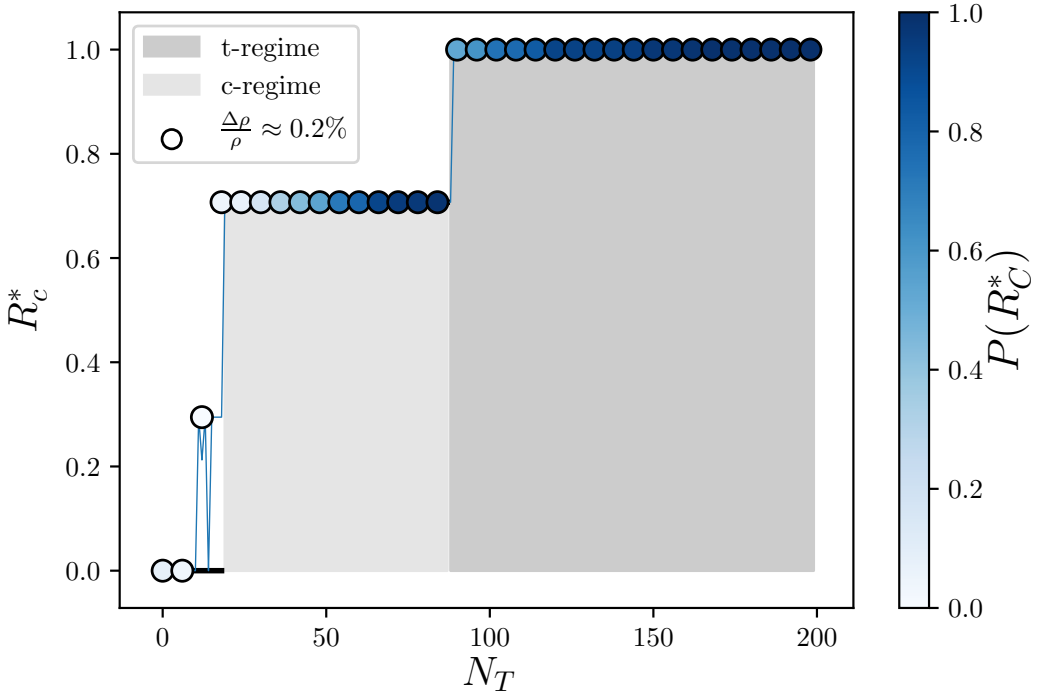

Figure S4: Influence of noise in the prediction of the average congestion radius R_c as a function of N_T, the number of nodes of the trees, with fixed branching factor $r = 2$ and grid width $w = 25$, and a noise level of 0.2%. Values are averaged over an ensemble of $n = 150$ realizations of the GT-model. Solid black lines present regimes as predicted by Eq. (17). Circles present the experimental results after the addition of noise. Each circle is located at the statistical mode obtained with the distribution of R_c after the 150 realizations. The color of the circle shows the probability of that value over the experimentally obtained distribution of R_c.

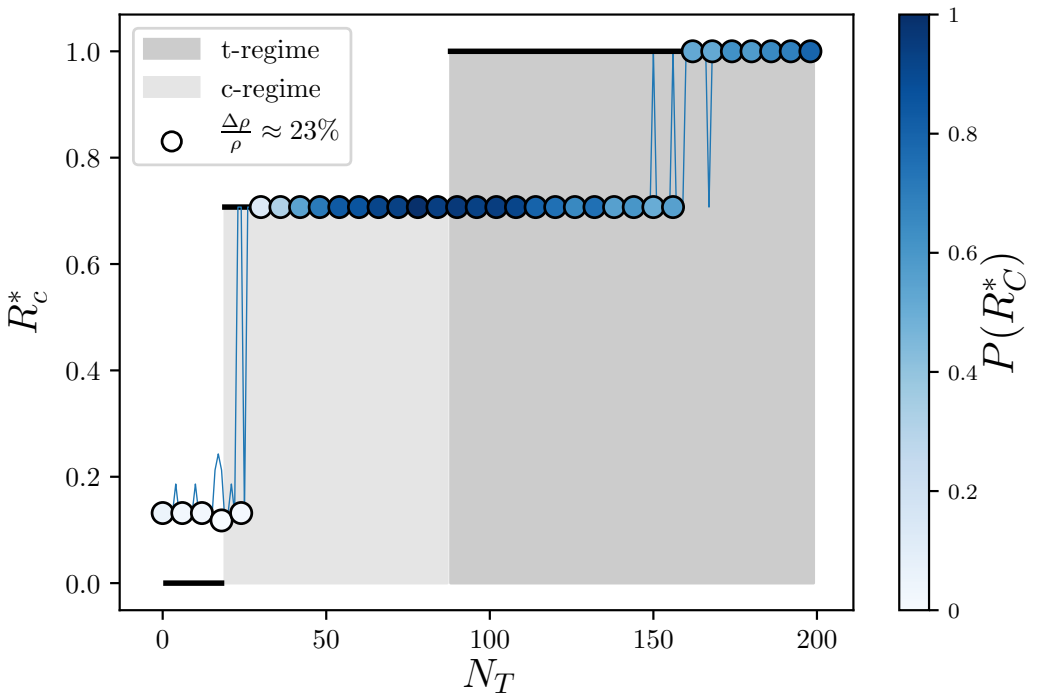

Figure S5: Influence of noise in the prediction of the average congestion radius R_c as a function of N_T, the number of nodes of the trees, with fixed branching factor $r = 2$ and grid width $w = 25$, and a noise level of 23%. Values are averaged over an ensemble of $n = 150$ realizations of the GT-model. Solid black lines present regimes as predicted by Eq. (17). Circles present the experimental results after the addition of noise. Each circle is located at the statistical mode obtained with the distribution of R_c after the 150 realizations. The color of the circle shows the probability of that value over the experimentally obtained distribution of R_c.

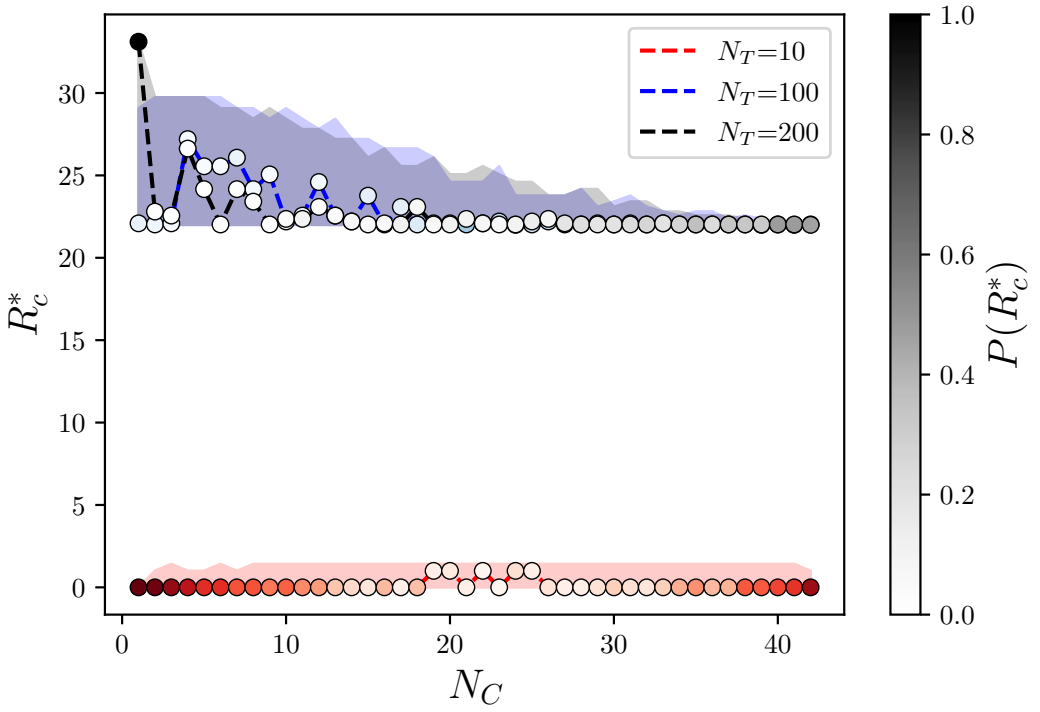

Figure S6: Dependence of the congestion radius on N_C, i.e., the number of peripheral trees connected to each side of the grid. All the trees are assumed to have the same number of nodes, and the point in which they are connected to the grid side is randomly chosen. Each point is located at the statistical mode (here indicated by R_c^*) resulting from the R_c distribution after 100 graph realizations at fixed N_C, and its color provides the occurrence of the R_c^* value in the distribution. Shadow areas fill the space between the minimum and maximum value taken by the congestion radius over the ensemble. Trees are connected to a grid characterized by $w = 45$ and exhibit branching factor $r = 2$, while their number of nodes is presented in the legend. The N_T are chosen in order to cover the three regimes. It is possible to see that the difference between the value the congestion radius takes in the t and c-regimes vanishes as the number of connections grows. However, it is always possible to distinguish a congestion center regime and a peripheral one.

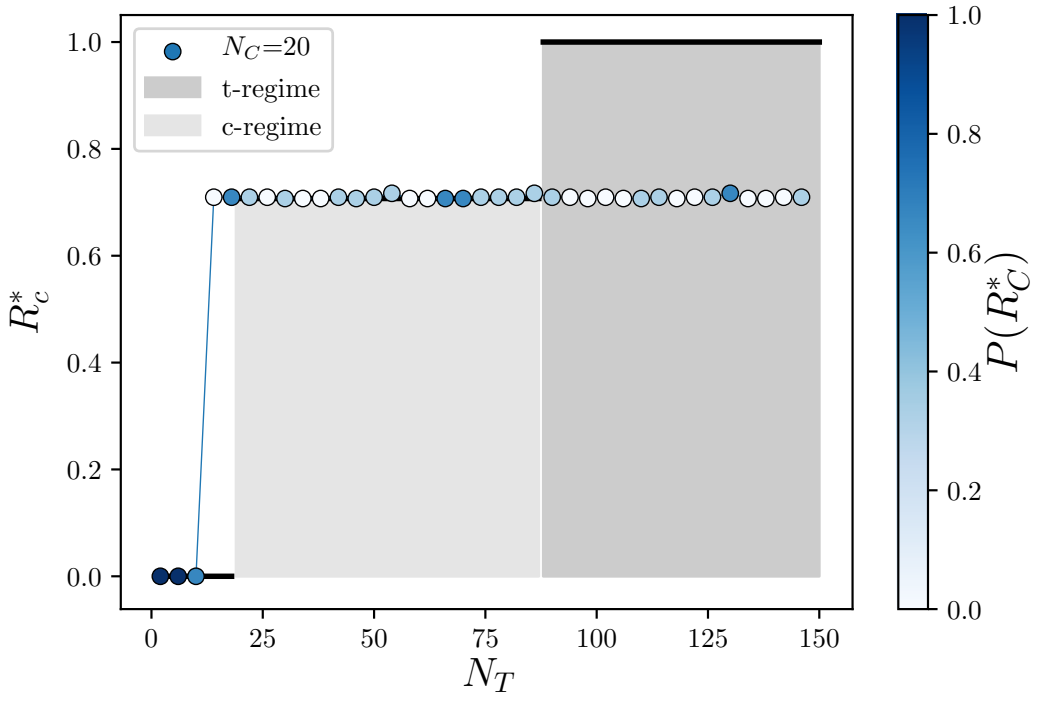

Figure S7: Dependence of the congestion radius on the number of tree nodes in the case of $N_C = 20$ peripheral trees. Trees are connected by the root to a random node of the grid perimeter. Each circle is located at the statistical mode (here indicated by R_c^*) resulting from the R_c distribution after 20 graph realizations at fixed N_C, and its color provides the occurrence of the R_c^* value in the distribution. Trees are connected to a grid characterized by $w = 25$ and branching factor $r = 2$. The t and c regimes are not distinguishable through a measure of the congestion radius for any value of N_T, however the abrupt transition between the g and c regimes still holds.

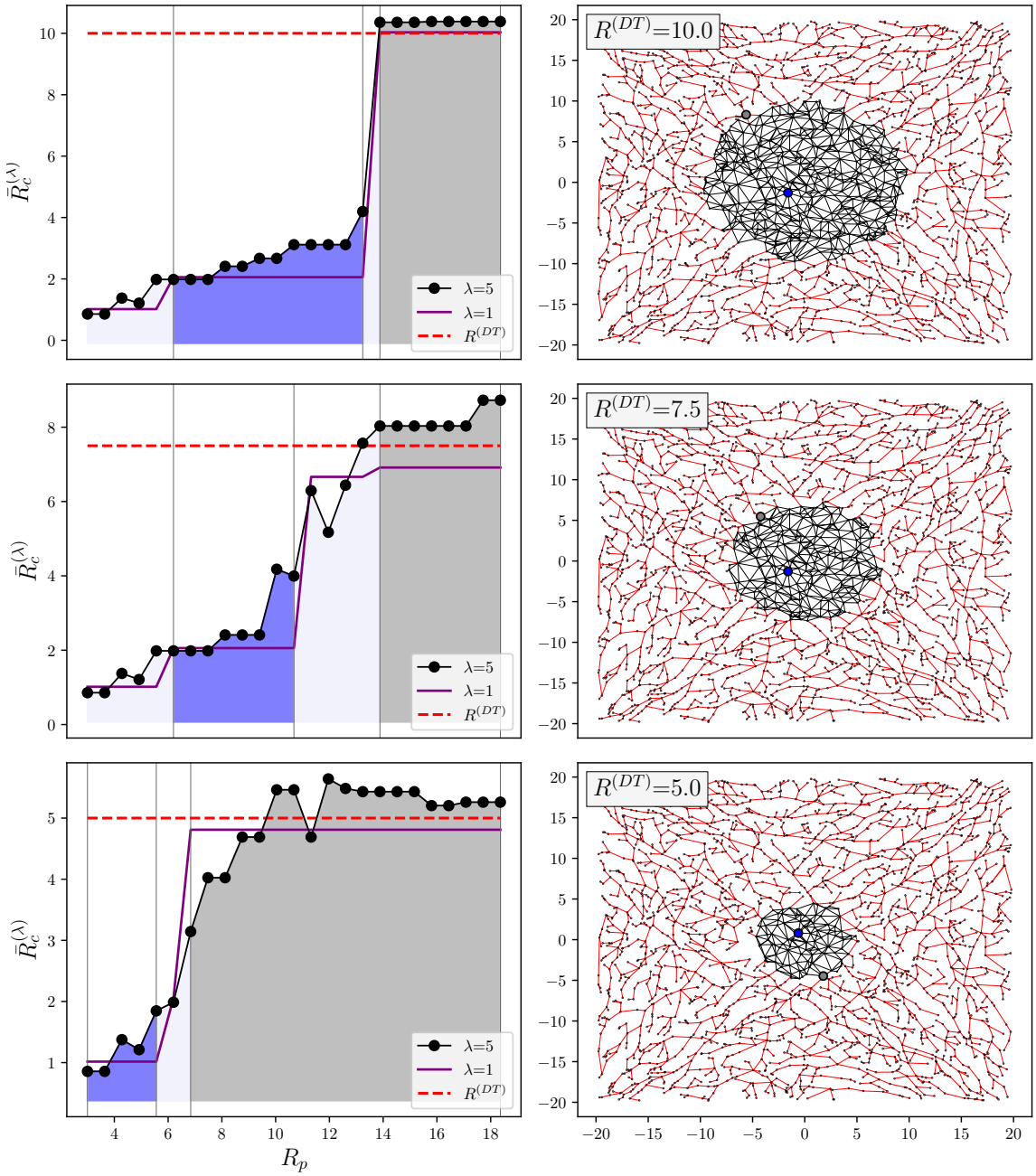

Figure S8: Spatial behavior of the congestion nodes for different configurations of the random planar model. Nodes number is equal to $N = 2400$, and their location follows a random uniform distribution. The left column shows the dependence of the congestion radius, evaluated by means of the quantity $\bar{R}_c^{(\lambda)}$ introduced in Eq. (19), as a function of the patch radius. The horizontal red dashed line represents the value of R^{DT}, separating the DT area from the MST one. In the right column we depict the corresponding network configuration, where DT and MST edges are painted in red and black, respectively. Grey and blue points are the first and second more frequent congestion nodes emerging for all the patches, and the corresponding patch radius range is painted with the same color in the left column.

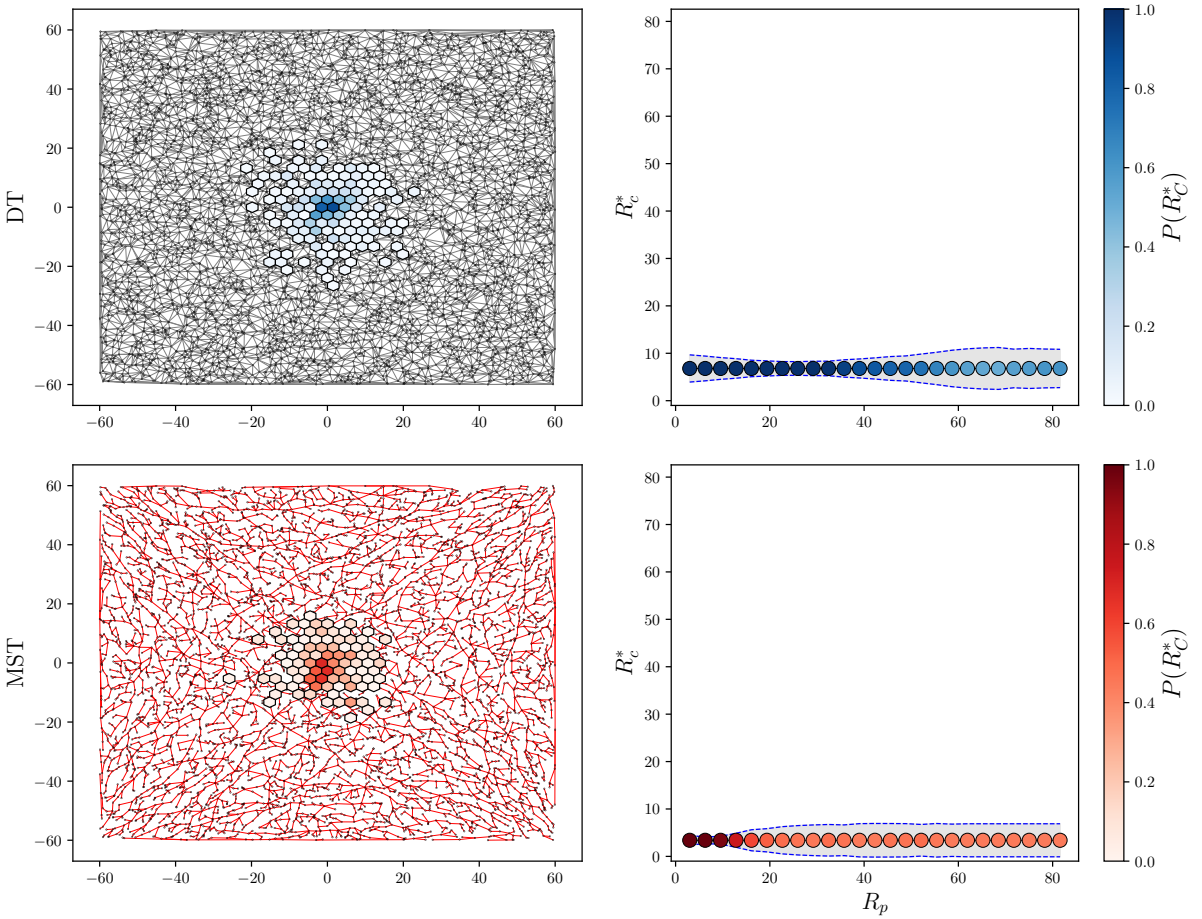

Figure S9: Spatial behavior of the congestion nodes for the DT (top) and the MST (bottom). The location of the nodes is completely random. The figure is organized similarly to Fig. 6: left column shows the network configuration, where hexagonal bins describe the occurrence of congestion in space, and right column presents the dependence of congestion radius on the patch radius. Here, circles are located at the statistical mode over an ensemble of 100 realizations of different random distributions of $N = 6000$ nodes in a square of side equal to $\ell = 60$. Importantly, congestion mostly occurs in the center and no transitions arise, suggesting that these are a consequence of the intertwining of different graph structures.

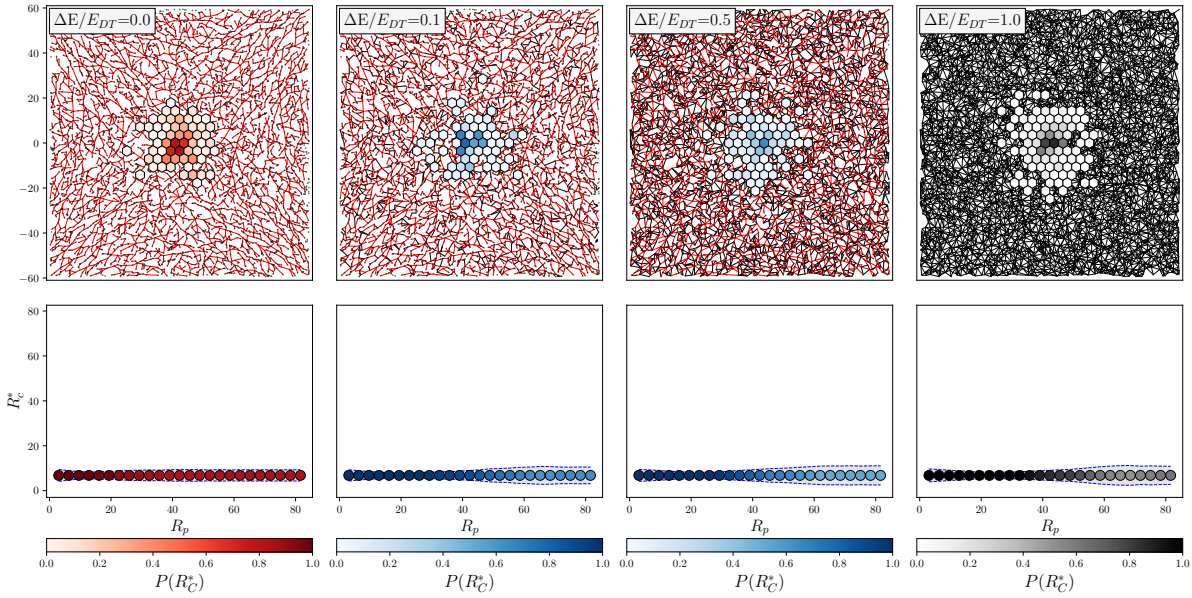

Figure S10: Spatial behavior of the congestion nodes for random planar models without any spatial separation between DT and MST. A DT is calculated for all the randomly located nodes, then its MST based on edge betweenness is found, and all the edges of this MST are included in the network. From all the DT edges not in the MST, a randomly selected fraction $\Delta E/E_{DT}$ is also added to the network (Delaunay noise, as explained in Appendix A). The figure is organized in the same manner as Fig. 6: top row shows the network configuration, where hexagonal bins describe the occurrence of congestion in space, and bottom row presents the dependence of congestion radius on the patch radius. Here, circles are located at the statistical mode over an ensemble of 100 realizations of the edge noise over the same random node distribution of $N = 6000$ nodes in a square of side equal to $\ell = 60$. Still, similarly to Fig. S9, congestion mostly occurs at the center and no transitions arise, suggesting that the spatial separation between DT and MST is a necessary condition for them.

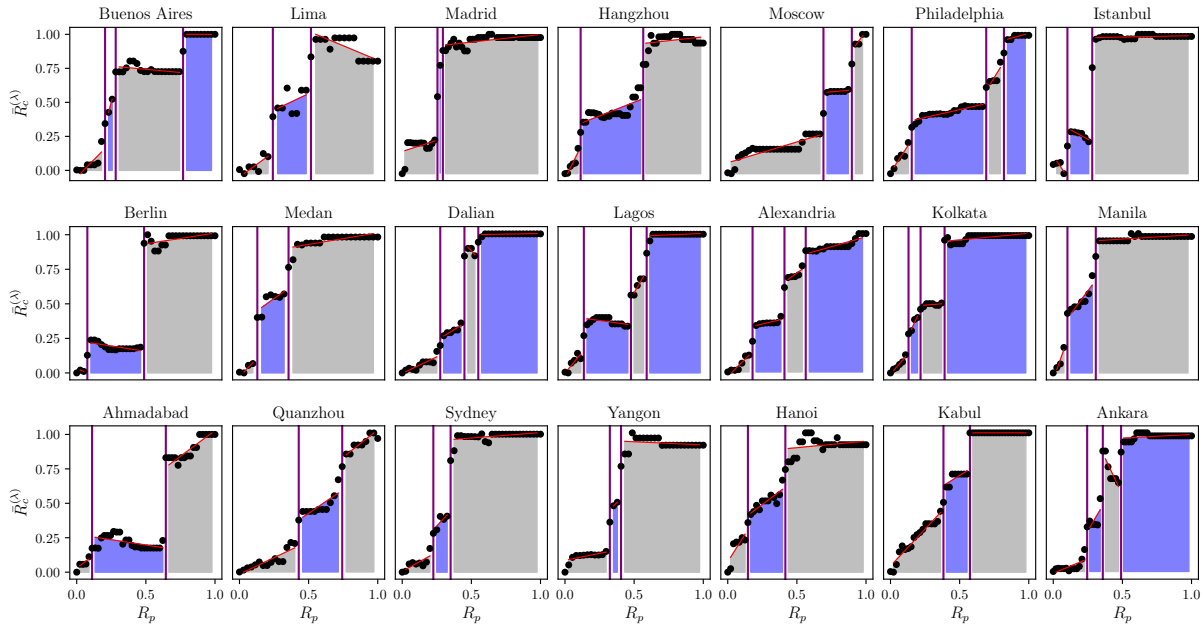

Figure S11: Additional analysis of congestion regimes on a set of 21 cities. Each point in the different plots represents the average distance from city center of the $\lambda = 15$ maximum betweenness nodes. Vertical lines indicate the change points, i.e., where either the mean or the slope of the congestion radius changes. Plots are normalized between 0 and 1 considering the radius of the different cities.

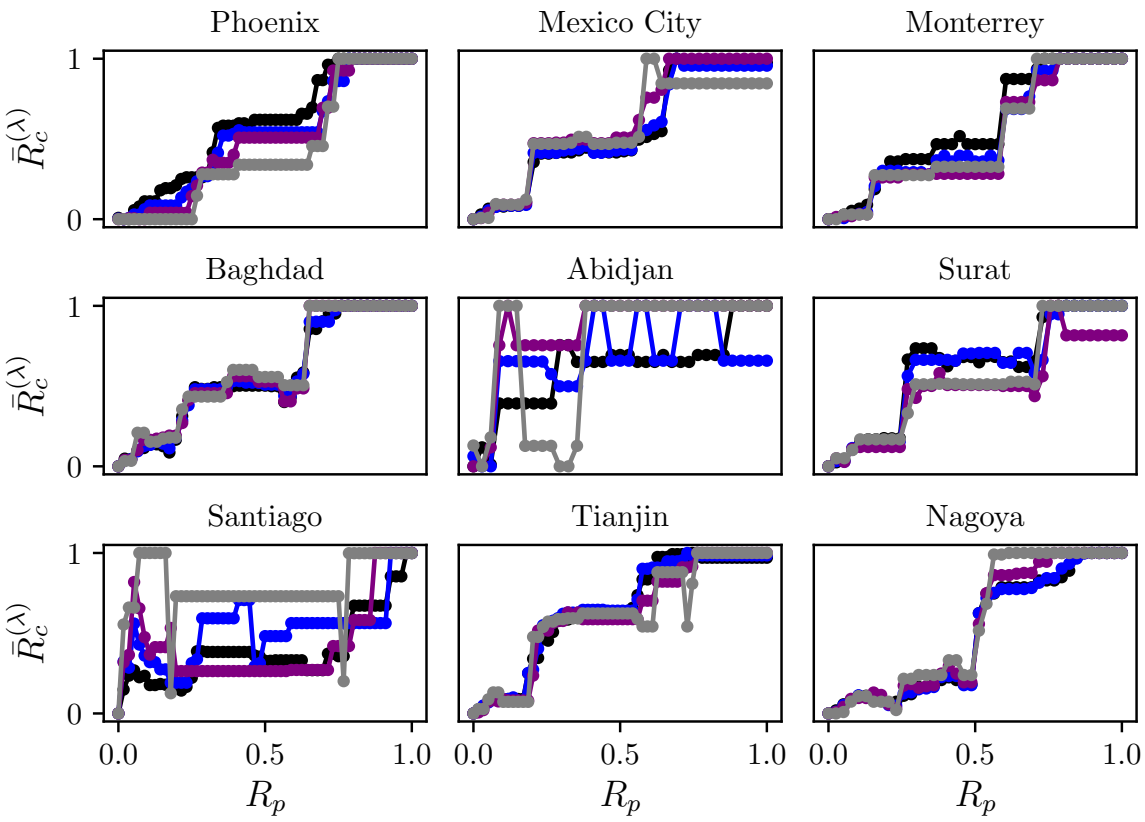

Figure S12: Analysis of the congestion regimes on several cities depending on λ. Points represent the average distance from city center of the λ maximum betweenness nodes: black line $\lambda = 15$; blue line $\lambda = 10$; purple line $\lambda = 5$; grey line $\lambda = 2$.

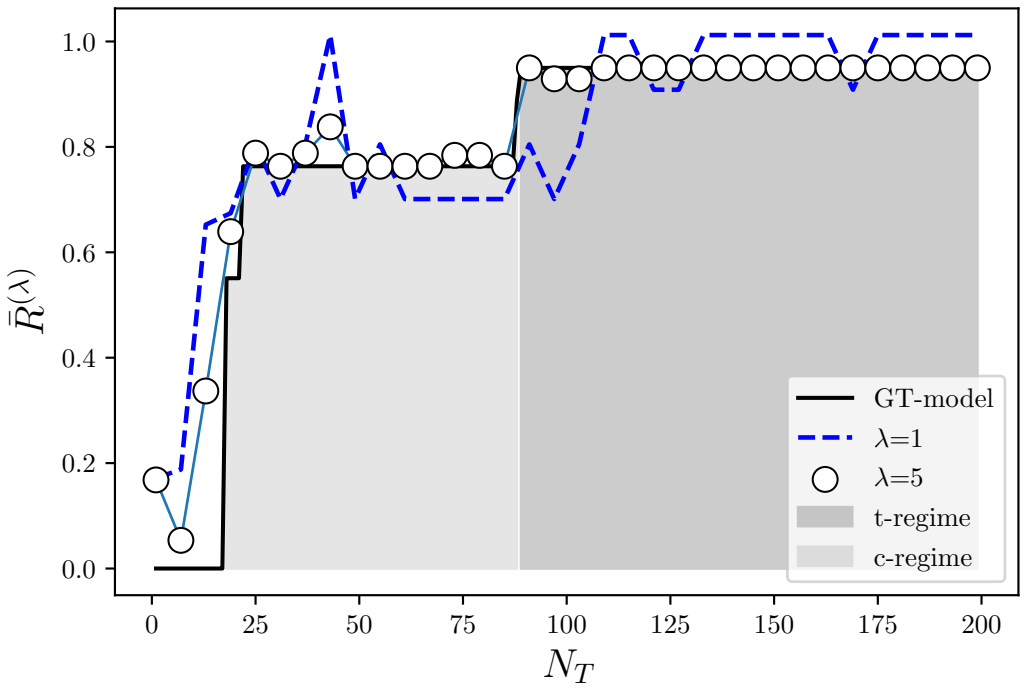

Figure S13: Validation of the quantity $\bar{R}^{(\lambda)}$ introduced in Eq. (19) on the GT-model, with fixed values of the branching factor $r = 2$ and grid width $w = 25$, as a function of the number of nodes of the trees, N_T. Solid black line refers to the GT-model without noise, while circles present the experimental results after the addition of noise with $\Delta\rho/\rho = 0.2\%$. In these two cases, the value of λ is set to be equal to 5, while the blue dashed line represents the same noisy behavior with $\lambda = 1$. In particular, we consider $n = 20$ realizations of the biased edge addition noise. Here, the final value of $\bar{R}^{(\lambda)}$ is averaged over these realizations. It results that the employ of $\bar{R}^{(\lambda)}$ preserves the abrupt transitions pattern detected by means of the R_c distribution mode, as shown for instance in Figs. S4 and S5. The difference between the values of $\bar{R}^{(\lambda)}$ in c and t regimes gets smaller as λ increases; this may be understood since, for $\lambda \geqslant 8$, the definition in Eq. (19) covers both the tree roots and middle-side grid nodes.